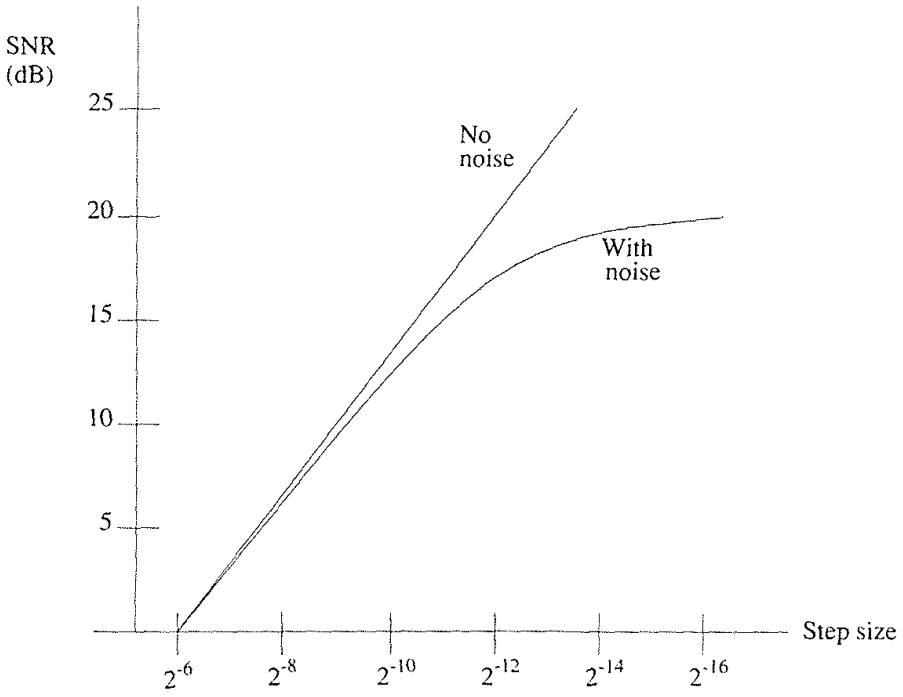

Fig. 9.17 SNR (desired distant signal to echo+noise) vs. asymptotic step size [16].

After $(2N+1)$ adaptation steps, the $(2N+1)$-tap transversal filter has had $(2N+1)$ successive tap voltage vectors $\mathbf{d}_n$ which, with high probability, are (algebraically) linearly independent. They span a $(2N+1)$-dimensional signal space and can be used as a basis to represent any vector in that space. The Kalman algorithm is an (implicit) Gram-Schmitt orthogonalization that (implicitly) builds a set of basis vectors that can represent a $\mathbf{c}_{opt}$ minimizing the accumulated squared error. If the $(2N+1)$ tap voltage vectors are not linearly independent, then "wait a little longer," and convergence is in mean-square for an arbitrary "random" input.

Following the development in Section 8.5 and referring to the notation of Figure 9.16, we assume a transversal (tapped delay line) filter with $(2N+1)$ taps. At the nth iteration, the tap weight vector is $\mathbf{c}_n$, with components c_{nj}, and the output of the canceler filter is

$$y_n = \mathbf{c}_n' \mathbf{d}_n = \sum_{k=-N}^{N} c_{nk} d_{n-k} . \tag{9.43}$$

At this iteration, the least squares estimate of the echo channel $\mathbf{h}_e$ is that which selects the tap weight vector $\mathbf{c}_i$ such that

$$S_n = \sum_{j=0}^{n} w_j e_j^2 , \tag{9.44}$$

is minimized, where the $\{w_j\}$ are a set of weights, ordinarily heavier for recent

than for old errors. A typical weighting is

$$w_j = \Delta^{n-j} , \tag{9.45}$$

where Δ is a positive number slightly less than one. The error e_j in (9.44) is given by

$$e_j = r_j - \mathbf{c}_n' \mathbf{d}_j , \tag{9.46}$$

where r_j is the received signal sample, including the echo component. Note that the tap weight vector used to define e_j is the latest one, not the tap weight vector that was available at the jth iteration. Thus e_j would have to be recomputed, for all j, $0 \le j \le n$, at each iteration, if it were used in the tap adjustment algorithm, which it is not.

The minimum of S is found from the $(2N + 1)$ equations resulting from equating the partial derivatives of S (with respect to the tap weights c_{nk}, $k = -N,\ldots, N$) to zero:

$$0 = \partial S/\partial c_{nk} = 2 \sum_{j=0}^{n} w_j d_{j-k} \left[r_j - \sum_{\ell=-N}^{N} c_{n\ell} d_{j-\ell} \right] , \quad -N \le k \le N ,$$

or

$$\sum_{j=0}^{n} \Delta^{n-j} r_j d_{j-k} = \sum_{\ell=-N}^{N} c_{n\ell} \sum_{j=0}^{n} \Delta^{n-j} d_{j-\ell} d_{j-k} , \quad -N \le k \le N . \tag{9.47a}$$

In vector format, (9.47a) may be written as

$$\sum_{j=0}^{n} \Delta^{n-j} r_j \mathbf{d}_j = \left[\sum_{j=0}^{n} \Delta^{n-j} \mathbf{d}_j \mathbf{d}_j' \right] \mathbf{c}_n . \tag{9.47b}$$

This is a set of n linear equations for the $(2N+1)$ elements of $\mathbf{c}_n$. When n reaches $2N+1$, and if the linear independence property holds, it should be possible to unambiguously represent $\mathbf{c}_{opt}$. Solving for $\mathbf{c}_n$,

$$\mathbf{c}_n = R_n^{-1} \sum_{j=0}^{n} \Delta^{n-j} r_j \mathbf{d}_j , \tag{9.48}$$

where

$$R_n = \sum_{j=0}^{n} \Delta^{n-j} \mathbf{d}_j \mathbf{d}_j' . \tag{9.49}$$

As in Chapter 8, the object is to use a recursive algorithm for $\mathbf{c}_n$ in order not to have to calculate $\mathbf{c}_n$ from (9.48) each iteration. Noting that

$$R_n = \Delta R_{n-1} + \mathbf{d}_n \mathbf{d}_n' \tag{9.50}$$

and using the matrix inversion lemma, and Kalman gain vector given by equations (8.88) and (8.89) of Chapter 8 (with α replaced by Δ and $\mathbf{r}_n$ replaced by $\mathbf{d}_n$), we arrive at the recursion relationship

$$\mathbf{c}_n = \mathbf{c}_{n-1} - e_n \mathbb{K}_n \tag{9.51}$$

by the steps outlined in Chapter 8 to derive (8.95). Here the Kalman gain vector is

$$\mathbf{K}_n = \frac{R_{n-1}^{-1}\,\mathbf{d}_n}{\Delta + \mathbf{d}_n'\,R_{n-1}^{-1}\,\mathbf{d}_n}. \tag{9.52}$$

At each iteration, the Kalman gain is recomputed (using the matrix inversion lemma (8.88) to update R_{n-1}^{-1}) and used in (9.51) to generate the new $\mathbf{c}_n$.

Some results using the Kalman algorithm are given in Section 9.4.1.

9.3.6 DATA-DRIVEN ECHO CANCELLATION: THE FRACTIONALLY-SPACED CANCELER

We noted earlier that echo canceler output samples are needed at Nyquist intervals rather than at symbol intervals if the local receiver is unsynchronized with the local data transmitter. If the echo canceler, locked to the local transmitter's clock, can produce outputs at Nyquist intervals, an interpolator can derive samples at the sampling times, locked to the distant transmitter, demanded by the local receiver.

A line-signal-driven echo canceler satisfies this requirement, but at a formidable cost in complexity. In a digital implementation, if there are M taps, at Nyquist intervals T', to span the echo channel dispersion, the filtering operation $\mathbf{c}_n'\mathbf{s}_A(n)$ requires (for a real baseband canceler) M multiplications and additions each T' seconds. The filtering multiplications, if done digitally, will involve tap weights c_{nm} of about 12 bits precision and tap voltages of about 8 bits precision (see Chapter 10).

The updating operation in the stochastic adaptation algorithm,

$$\mathbf{c}_{n+1} = \mathbf{c}_n + \beta e_n \mathbf{s}_A(n), \tag{9.53}$$

similarly requires M multiplications and additions, so that there is a total of $2M$ multiplications and additions per Nyquist interval. If the variables used above represent an equivalent (complex) baseband model of a passband canceler, as would actually be the case in practice, the number of real multiplications is four times as large. Thus there could be $8M$ high-precision multiplications per T' interval. If T' were one-fourth the symbol interval T, as it may be in practice, there would be $32M$ multiplications per symbol interval T, or $32M/T$ multiplications per second. With $N = 128$ taps and $T = 1/2400$ sec, the requirement would be close to 10 million high-precision multiplications per second.

The severity of this requirement stimulated development of *data-driven* echo cancelers, as described in the previous section, in which outputs are computed only at symbol intervals and the multiplications are simpler because tap voltages are restricted to a very few values, e.g., two if the data are binary [18]. The echo canceler replicates the combination of transmitter filter and echo channel. But this solution does not provide samples at Nyquist intervals, and requires synchronization of the two transmitters. Fortunately techniques have

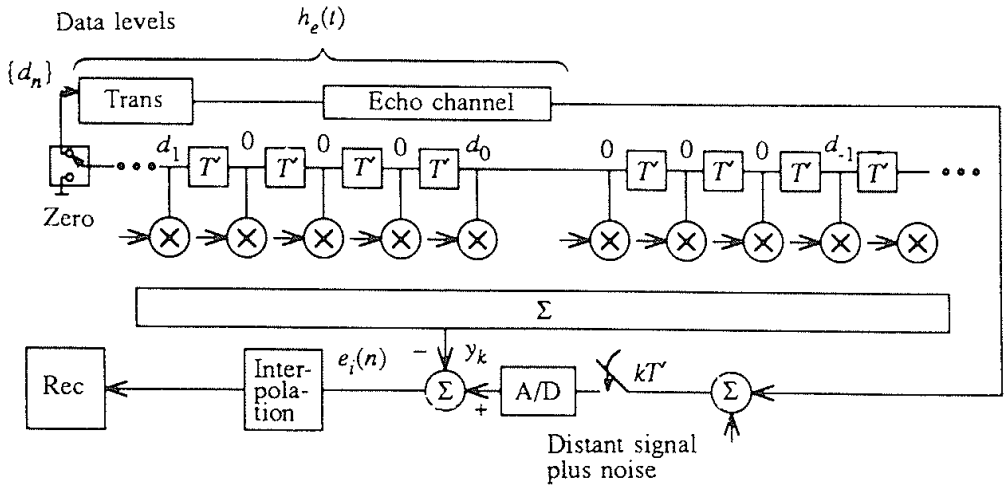

Fig. 9.18 Fractionally-spaced echo cancellation, illustrated for $T' = T/4$. Adaptation is not shown.

been found to simultaneously obtain most of the advantages of both data-driven and unsynchronized (Nyquist-interval) cancellation techniques [16,19]. The number of multiplications, as well as the complexity of each multiplication, is substantially reduced from the requirements of a straightforward line-signal-driven Nyquist-interval canceler.

As shown in Figure 9.18, the canceler is similar to that of Figure 9.13 (for the line-signal-driven model) in that it updates tap weights at Nyquist intervals T' that are a fraction of T, but the reference signal driving the canceler is the data train feeding the local transmitter rather than the line signal produced by the local transmitter. Since data occur only at symbol intervals T, the reference signal driving the canceler at intervals T' is nonzero only part of the time. If $T' = T/4$, then only one in four reference signal inputs to the canceler is nonzero. We will show that this structure produces exactly the same echo estimates as the line-signal-driven canceler which had nonzero inputs every T' seconds. The Nyquist-interval outputs, locked to the local data transmitter, are interpolated, as described above, to produce samples at the times desired by the local receiver.

This fractionally-spaced canceler retains the computational simplicity of the symbol-interval data-driven echo canceler, with arithmetic using a few data levels, and most reference inputs equal to zero. In fact, as we will show, it consists of ℓ interleaved symbol-interval cancelers, where $\ell = T/T'$. It allows complete independence of operation of the stations at the two ends of the line, just as with the line-signal-driven canceler.

To derive the structure of Figure 9.18, assume a received echo signal

$$r_e(t) = \sum_m d_m h_e(t - mT) \ , \qquad (9.54)$$

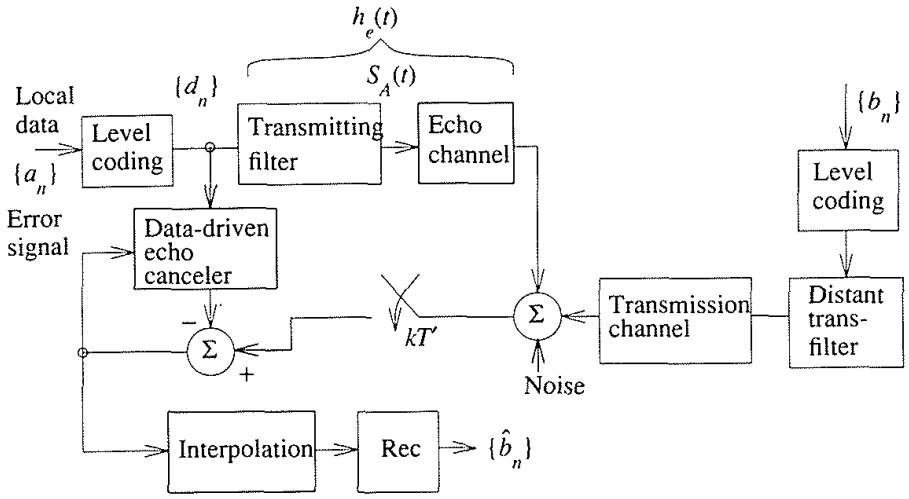

Fig. 9.19 System model for data-driven, fractionally-spaced echo cancellation.

where $\{d_m\}$ is the data train (modulation levels) feeding the local transmitter's pulse generator, and $h_e(t)$ is the overall echo channel, including the local transmitter filter, as shown in Figure 9.19.

At intervals T', samples of the received echo signal are

$$r_e(kT') = \sum_m d_m h_e(kT' - mT) \ . \tag{9.55}$$

Assuming $T' < 1/2f_{\max}$, where $f_{\max}$ is the highest frequency in $r_e(t)$, the sample train is sufficient to determine $r_e(t)$ for *any* value of t.

Suppose that

$$T' = T/\ell \ , \tag{9.56}$$

where ℓ is an integer, e.g., $\ell = 4$. Then

$$r_e(kT') = \sum_m d_m h\left[(k - m\ell)\,T'\right] \ , \tag{9.57a}$$

and defining $h_k = h_e(kT')$,

$$r_e(kT') = \sum_m d_m h_{k-m\,\ell} \ . \tag{9.57b}$$

This echo-channel convolution can be duplicated in an infinite transversal filter with tap weights ($c_i = h_i$). Note in (9.57) that only every ℓth tap weight is used. Different sets of tap weights, spaced ℓ taps apart in each case, are used for $k = 0, k = 1, \ldots, k = \ell - 1$. For $k + \ell$, $r_e((k + \ell)T')$ requires the same set of tap weights as for computing $r_e(kT')$, but with the data shifted to the right. These operations can be realized by the "zero stuffer" canceler shown in Figure 9.18.

What we effectively have is ℓ interleaved *symbol-interval* transversal filters corresponding to ℓ timing instants within a symbol interval. The ℓ cancelers are

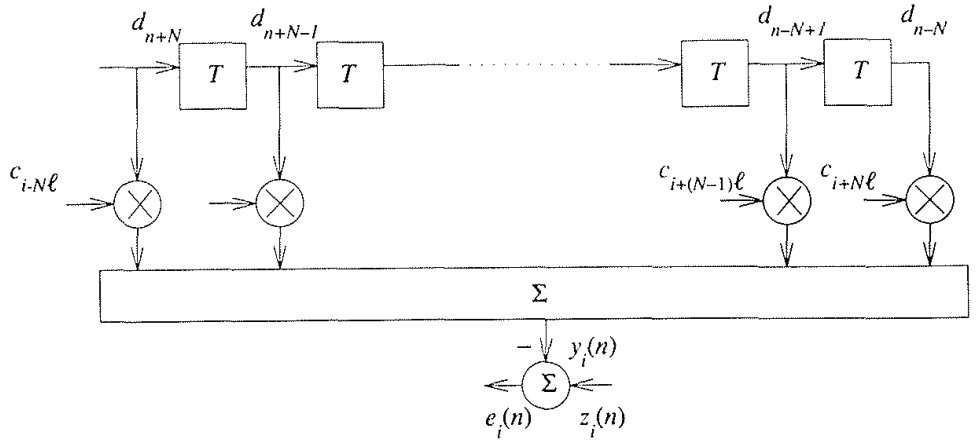

Fig. 9.20 Symbol-interval data-driven echo canceler, the ith subcanceler of the fractionally-spaced data-driven echo canceler.

operated and adapted independently. This becomes clearer with a further refinement of notation. Let

$$kT' = nT + iT' = (n\ell + i)T' , \tag{9.58}$$

where n is the largest multiple of T contained in kT', and $i = k \bmod(\ell)$. Let the echo replica be

$$\begin{aligned} y_i(n) = y(kT') &= \sum_m d_m c_{k-m\ell}(n) \\ &= \sum_{j=-N}^{N} d_{n-j} c_{i+j\ell}(n), \text{ all } n, i = 0,1,\ldots,\ell-1 . \end{aligned} \tag{9.59}$$

For each of the ℓ values of i, (9.59) describes a symbol-interval transversal filter (Figure 9.20) with $(2N + 1)$ tap weights.

Defining $\mathbf{c}_i(n)$ as the tap weight set that generates $y_i(n)$, with jth element $c_{i+j\ell}(n)$, and $\mathbf{d}(n)$ as the vector $(d_{n+N}, \ldots, d_{n-N})$ of data levels, (9.59) becomes

$$y_i(n) = \mathbf{c}_i'(n)\ \mathbf{d}(n) . \tag{9.60}$$

Each of the ℓ interleaved cancelers is updated once each symbol interval, according to the stochastic algorithm described in the previous section. Explicitly, the error in the output of the ith canceler at the nth symbol interval is

$$\begin{aligned} e_i(n) = \mathbf{h}_i'\mathbf{d}(n) &+ \mathbf{g}_i'\mathbf{b}(n) + \eta_{n\ell+i} - \mathbf{c}_i'(n)\mathbf{d}(n) , \\ &\text{echo sample at } t = (n\ell+i)T' \quad \text{received distant signal at } t = (n\ell+i)T' \quad \text{noise} \quad \text{echo replica} \end{aligned} \tag{9.61}$$

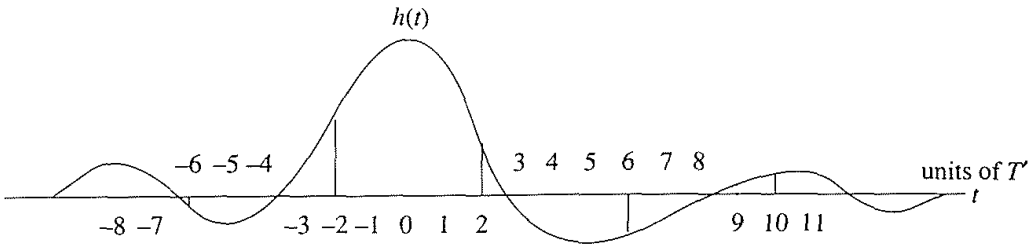

Fig. 9.21 Interleaved vectors of echo-channel samples for $\ell = 4$. h_i samples shown for $i = 2$.

where $\mathbf{g}_i$ represents the direct transmission channel from the distant transmitter to the local receiver, $\mathbf{b}(n)$ is the data vector at the distant transmitter, and

$$\mathbf{h}_i = h_e(iT' - NT), \ldots, h_e(iT' + NT), \quad i = 0,1,\ldots,(\ell - 1) \qquad (9.62)$$

is the ith of ℓ interleaved vectors of echo channel impulse response samples at symbol intervals (Figure 9.21).

The tap updating formula is, from (9.29),

$$\mathbf{c}_i(n+1) = \mathbf{c}_i(n) + \beta e_i(n)\mathbf{d}(n), \quad i = 0,\ldots,\ell-1.$$

Thus each symbol interval, each of the ℓ symbol-interval subcancelers, is updated according to the usual LMS algorithms. As with channel equalizers, it may be desirable to use a larger step size β at first for rapid convergence and a smaller one later for small residual error.

The convergence characteristics of the interleaved symbol-interval cancelers may vary to some extent, because the covariance matrices of the ℓ symbol-interval sampled echo channels may differ significantly. However, in practice, the convergence characteristics are similar. Figure 9.22 illustrates convergence from simulation experiments using a typical echo channel characteristic.

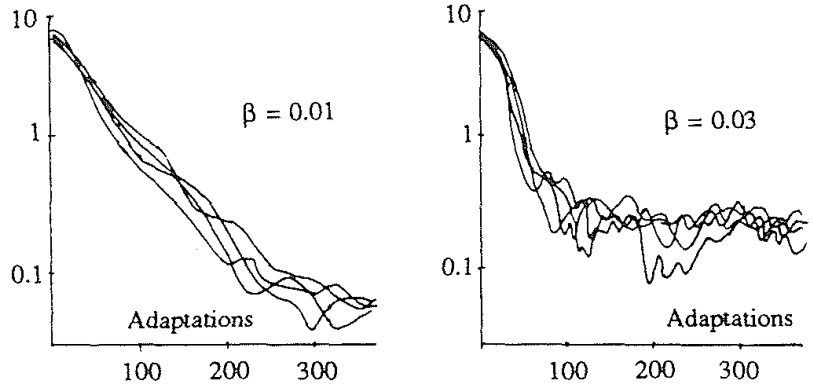

Fig. 9.22 Simulation runs, at two step sizes, for convergence of the four interleaved symbol-interval subcancelers of a fractionally-spaced echo canceler with two 10-tap "near" and "distant" echo sections, operating on the echo channel $h_e(t) = h_0(t-t_a) + h_0(t-t_b)$. Noise was present at a level 10 dB below the total echo power.

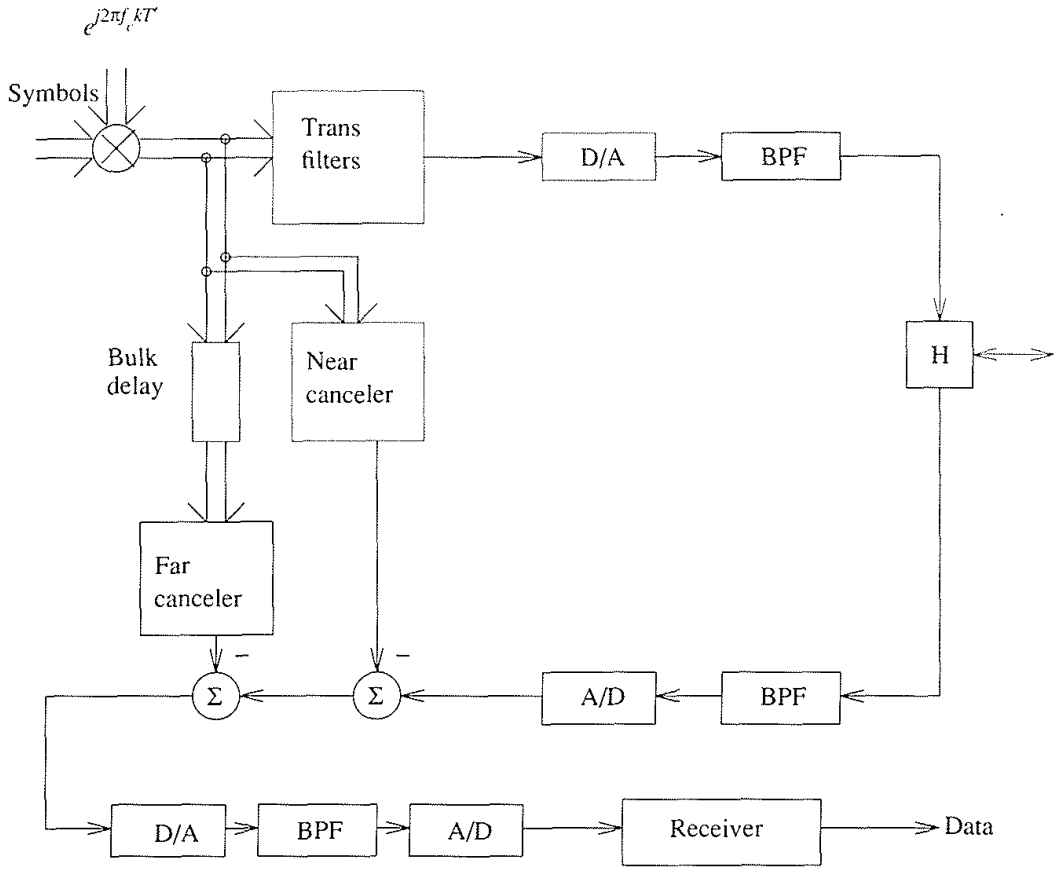

Fig. 9.23 A digital realization of a fractionally-spaced echo canceler [14].

For digital implementations, digital resolution and high accuracy in analog to digital converters are essential. Figure 9.23 shows an implementation [16] in which passband cancellation and receiver operations are done in the digital domain. However, the interpolation between the Nyquist-interval samples generated at the canceler output, clocked by the local transmitted data stream, and the symbol-interval samples required by the receiver, which is clocked by the distant transmitted data stream, is achieved by D/A conversion of the clean Nyquist-interval sample stream, conversion to a continuous analog waveform in a bandpass filter, and sampling by the receiver with the timing epoch recovered from the received data. It has been found [20] that considerably more digital resolution is required in the tap weights than in the tap voltages, in order to allow tap updating sufficient to reduce the mean-square cancellation error to an acceptable level. These and related considerations of digital resolution are described in Chapter 10.

9.3.7 ADAPTIVE REFERENCE ECHO CANCELLATION

We have noted that the desired distant signal is a component of the noise as far as adaptation of the local echo canceler is concerned. It is included in the

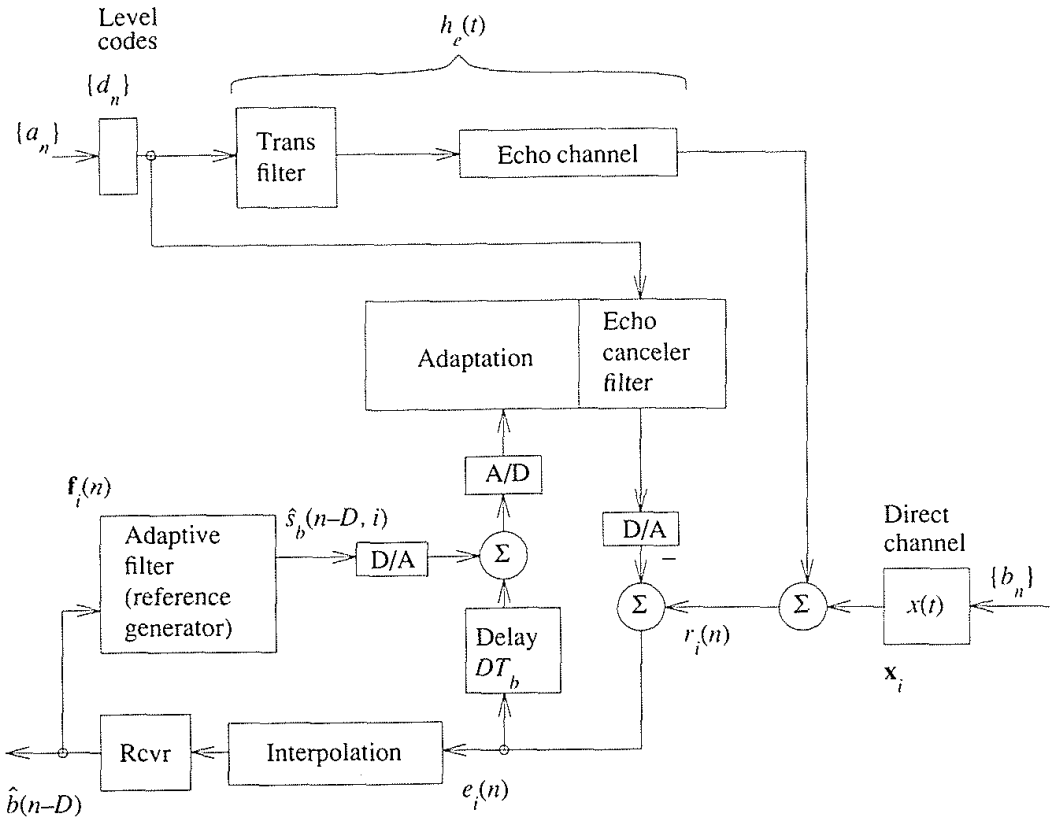

Fig. 9.24 Adaptive-reference echo cancellation (adapted from Falconer [21]).

"noise" variance of expression (9.42) for the residual mean-square cancellation error. This is a major performance disadvantage, but cancelers which treat the desired distant signal as part of the noise do have the advantage of avoiding all coordination between the near and distant transmitters (other than assuring that their signals are uncorrelated).

In principle, however, it should be possible to subtract out an estimate of the desired distant signal from the error signal $e(n)$ used to adapt the echo canceler, so that the echo canceler does not have to work against the large "noise" represented by the desired distant signal. In a symbol interval canceler, with adequate synchronization capabilities, this is possible with an adjunct decision feedback equalizer, generating a replica at symbol intervals of the precursor interference. If a delay in canceler adaptation is accepted, the "precursors" can include almost all significant pulse samples, allowing almost total elimination of the distant signal from the canceler error signal.

D. D. Falconer [21] extended these ideas to Nyquist-interval cancellation, yielding the advantages of adaptive-reference echo cancellation without requiring synchronization of the two transmitters.

To see how it works, consider the system diagram of Figure 9.24. Assume, as in the last section, an echo channel with $2NT$ dispersion represented by vec-

tors

$$\mathbf{h}_i = h_e\left([i/\ell]T - NT\right), \ldots, h_e\left([i/\ell]T + NT\right), \quad i = 0, \ldots, (\ell - 1), \tag{9.63}$$

where the index i corresponds to one of ℓ sampling phases in a symbol interval T. This echo channel is replicated in the echo cancellation filters $\mathbf{c}_i$ in Figure 9.24. Similarly, the direct transmission channel $x(t)$, represented by $(2N + 1)$-dimensional vectors

$$\mathbf{x}'_i = x\left([i/\ell]T - NT_b\right), \ldots, x\left([i/\ell]T + NT_b\right), \quad i = 0, \ldots, (\ell - 1), \tag{9.64}$$

is replicated in the reference generator filters $\mathbf{f}_i$. Here T_b is used instead of T to make clear that the symbol rate T_b at the distant transmitter may differ slightly from the symbol interval T at the local transmitter.

The subtraction of the reference signal emerging from the $\mathbf{f}_i$ operations from the cancellation error signal is done in the analog domain with interpolated waveforms, thereby avoiding any concern over lack of synchronization (including a possible small difference of T_b from T) between the two transmitters. Analog subtraction also avoids high-resolution requirements for digital subtraction in cases where the distant signal has considerably lower energy than the echo signal.

The delay of D symbol intervals for the error signal $e_i(n)$, before the reference signal is subtracted from it and the result is used to adapt the echo canceler, corresponds to the processing delay in the local receiver. That is, the estimate of the distant data symbol b_n is not available until DT_b seconds after the pulse on which it is modulated appears at the receiver input. If the echo channel is constant or slowly varying, this delay in adaptation of the echo canceler is generally not a problem. (See Chapter 10 for a quantitative discussion of the effect of delay on the LMS algorithm.)

The reference signal output sample at time $t = (n + i/\ell)T_b$ is given by

$$\hat{s}_b(n - D, i) = \sum_{k=-N}^{N} b(n - D - k)\, f_i(k) . \tag{9.65}$$

The delayed error signal is

$$e_i(n) = \mathbf{b}'(n - D)\, \mathbf{V}_i(n) + \mathbf{d}'(n - D)\, \mathbf{U}_i(n - D) + \mathrm{v}_i(n - D), \tag{9.66}$$

where

$$\mathbf{v}_i(n) = \mathbf{x}_i - \mathbf{f}_i(n) \tag{9.67}$$

is the error in the filter replicating the direct channel, and

$$\mathbf{U}_i(n) = \mathbf{h}_i - \mathbf{c}_i(n) \tag{9.68}$$

is the error in the filter replicating the echo channel. The index n is actually different in (9.67) and (9.68), clocked to T_b for the former and T for the latter, but it is not a critical distinction in actual operation, implying only that updatings are made at slightly different times in $\mathbf{c}_i$ and $\mathbf{f}_i$.

A stochastic adaptation algorithm follows immediately from these considerations. Squaring $e_i(n)$ and taking the derivatives with respect to elements of the echo cancellation and reference generation filters, and using these as estimates of the gradient, the adaptation algorithm is

$$\begin{aligned} \mathbf{f}_i(n+1) &= \mathbf{f}_i(n) + \beta_1\, e_i(n)\, \mathbf{b}(n-D) \\ \mathbf{c}_i(n+1) &= \mathbf{c}_i(n) + \beta_2\, e_i(n)\, \mathbf{d}(n-D)\ , \end{aligned} \tag{9.69}$$

where β_1 and β_2 are step sizes. Algorithm (9.69) presumes, just as for data-driven channel equalization (Chapter 8), that the decisions $b(n)$ are correct, but occasional errors will not seriously degrade adaptation.

An examination of convergence of one of the symbol-interval filter pairs $(\mathbf{f}_i, \mathbf{c}_i)$ is sufficient to describe convergence of the entire fractionally-spaced structure. It is shown in [21] that the mean tap weight error $E\{\mathbf{U}_i(n)\}$ converges exponentially to zero with n for $0 < \beta_2 < 1$ and $D = 0$, and shows a sampled oscillatory convergence to zero for moderate values of β_2 and nonzero integer values of the delay D. A stable value for the mean tap-weight error vector is achieved for $0 < \beta_2 < 0.2$ and $0 \le D \le 8$. The mean-square error, $E\{|\mathbf{U}_i(n)|^2\}$, converges at a rate independent of the sampling phase i and of the channel and echo impulse responses, just as for the zero reference echo cancellation systems of previous sections. The rate of convergence is related in a complicated way to the step sizes, delay D, and dispersion lengths of the direct and echo channels. The asymptotic (steady-state) mean-square error is

$$E\left\{|\mathbf{U}_i(n)|^2\right\} = \frac{\beta_2 N_e \sigma_v^2}{2 - \left(\beta_1 N_h + \beta_2 N_e\right)} \tag{9.70}$$

where N_e is the length (symbol-interval samples) of the echo channel, and N_h is the length of the direct channel. Figure 9.25 compares the convergence and steady-state error performance of zero reference and adaptive reference cancellation algorithms respectively in a typical system, assuming $N_e = N_h$.

9.3.8 FAST STARTUP ECHO CANCELLATION

We have seen, in the algorithms described in earlier sections, that the desired distant signal is part of the noise perturbing echo canceler operation and significantly slows convergence. This is a particularly severe problem during startup, when the tap weight errors are initially far away from their optimum values and convergence time may not be acceptable even with a large initial step

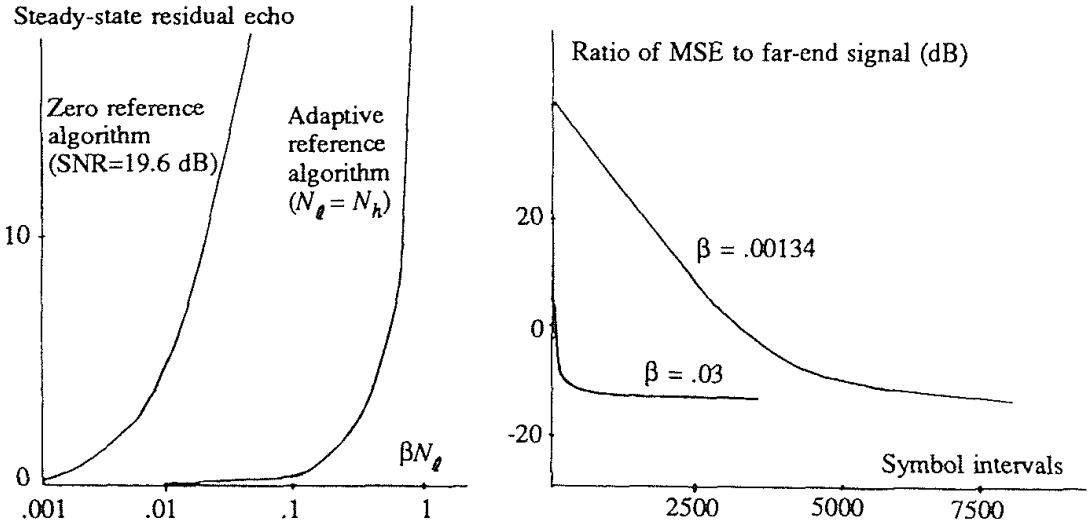

Fig. 9.25 (a) Relative steady-state residual echo vs. step size β for zero reference and adaptive reference cancelers respectively (SNR = 19.6 dB). (b) Convergence characteristics for zero reference and adaptive reference cancelers. (SNR = 15 dB, $N_e = 10$) (from Falconer [21]).

size. For this reason, a commonly used procedure for starting up an echo canceler is to do an initial adaptation in the absence of double-talking, i.e., with the distant transmitter quiet. Another practical procedure is to sound the echo channel and correlate the output with the input, as described in Section 9.3.1.

However, even with these procedures, startup is slower than desired in many applications. One approach to speeding it up is with the least squares adjustment algorithm of Section 9.3.5, which has the complexity costs described in that section. Alternatively, a modified stochastic adaptation algorithm discovered by Farrow and Salz exhibits performance comparable to the least squares algorithm, that is, adaptation in a number of iterations comparable to the length of the canceler filter, but with lower complexity comparable to the LMS algorithm.

Salz [31] motivates the procedure, with a pseudorandom (PN) sequence driving the transmitter filter and echo canceler of Figure 9.16. Recall (9.48), from Section 9.3.5, for the best estimator $\mathbf{c}_n$ of the tap weight set at the nth iteration of the least-squares adaptation algorithm. With the weighting $\Delta = 1$ in that equation, we have

$$\sum_{j=0}^{n} \mathbf{d}_j r_j = \left[\sum_{j=0}^{n} \mathbf{d}_j \mathbf{d}_j' \right] \mathbf{c}_n \ , \tag{9.71}$$

or

$$R_n \mathbf{c}_n = \mathbf{u}_n \ , \tag{9.72}$$

where

$$R_n = \sum_{j=0}^{n} \mathbf{d}_j \mathbf{d}_j' \quad \text{and} \quad \mathbf{u}_n = \sum_{j=0}^{n} \mathbf{d}_j r_j \ . \tag{9.73}$$

As in earlier sections, all vectors are of length $2N+1$, the span of the echo canceler. If the $\{d_k\}$ are random ± 1 data, and if one makes an assumption of ergodicity, so that time averages approach ensemble averages, then as $n \to \infty$, and recalling (9.12) for r_n,

$$\mathbf{u}_n \to n \ E\{\mathbf{d}_j r_j\} = n \ E\{\mathbf{d}_j \mathbf{d}_j'\} \mathbf{h}_e = n \mathbf{h}_e \tag{9.74a}$$

$$R_n \to n \ E\{\mathbf{d}_j \mathbf{d}_j'\} = nI \ . \tag{9.74b}$$

Thus from (9.72),

$$\mathbf{c}_n = R_n^{-1} \mathbf{u}_n \underset{n \to \infty}{\longrightarrow} \mathbf{h}_e \ , \tag{9.75}$$

the optimum tap weight vector yielding exact echo cancellation.

But for finite n, the statistical behavior of $\mathbf{c}_n$, and thus the progress of convergence, is hard to determine. The conditions on the random data sequence that would guarantee the existence of R_n^{-1} are not known. At a minimum, n has to be greater than $(2N + 1)$, for if it were not, the zero elements of $\mathbf{d}_n$ not yet occupied with data would result in all-zero rows and columns of R_n. The zero elements could be filled in with fake data, but there would be little point in adaptation with such a reference.

If an inverse of R_n exists, we can show that the tap weight estimator is unbiased. Specifically, from (9.14), (9.72), and (9.73), $r_j = \mathbf{d}_j' \mathbf{h}_e + \nu_j$,

$$\begin{aligned} \mathbf{c}_n = R_n^{-1} \ \mathbf{u}_n &= R_n^{-1} \left[\sum_{j=0}^{n} \mathbf{d}_j \mathbf{d}_j' \right] \mathbf{h}_e + R_n^{-1} \sum_{j=0}^{n} \mathbf{d}_j \nu_j \\ &= \mathbf{h}_e + R_n^{-1} \sum_{j=0}^{n} \mathbf{d}_j \nu_j \ , \end{aligned} \tag{9.76}$$

so that, with the data and noise uncorrelated,

$$E\mathbf{c}_n = \mathbf{h}_e \ . \tag{9.77}$$

To guarantee the existence of the inverse of R_n, we seek appropriate *fixed* data sequences. Assuming that such a sequence $\{d_j\}$ has been found, we can define an *error matrix*

$$M = E\left\{ (\mathbf{c}_n - \mathbf{h}_e) \ (\mathbf{c}_n - \mathbf{h}_e)' \right\} . \tag{9.78}$$

Substituting (9.76) into (9.78), and recalling that the noise variance is $E\nu_j^2 = \sigma_\nu^2$,

$$M = E\left\{R_n^{-1}\left[\sum_{j,k=0}^{n} \mathbf{d}_j \nu_j \nu_k \mathbf{d}_k'\right] R_n^{-1}\right\} = \sigma_\nu^2 R_n^{-1} . \tag{9.79}$$

The variance of the vector estimator $\mathbf{c}_n$ is the trace (sum of the diagonal terms) of the error matrix:

$$E\|\mathbf{c}_n - \mathbf{h}_e\|^2 = \text{trace } M = \sigma_\nu^2 \text{ trace } \left[\sum_{j=0}^{n} \mathbf{d}_j \mathbf{d}_j'\right]^{-1} . \tag{9.80}$$

As $n \to \infty$, the trace approaches zero. For any finite n, and any chosen data sequence, the variance $E\|\mathbf{c}_n - \mathbf{h}_e\|^2$ can be evaluated.

As candidates for a good fixed data sequence, consider two possible $(2N + 1)$-length $\pm$ data sequences, one orthogonal and the other pseudorandom. For the orthogonal sequence, which by definition has zero correlation with any time shift of itself, and $n = 2N + 1$, the ikth element of R_{2N+1} is

$$\left[\sum_{j=0}^{2N+1} \mathbf{d}_j \mathbf{d}_j'\right]_{ik} = \sum_{j=0}^{2N+1} d_{j-i} d_{j-k} = \begin{cases} 2N+1, & i = k \\ 0, & i \neq k \end{cases} \tag{9.81}$$

implying

$$E\|\mathbf{c}_n - \mathbf{h}_e\|^2 = \sigma_\nu^2 . \tag{9.82}$$

This is the best possible result, but it is not known how to construct an orthogonal sequence for any $(2N + 1)$. Pseudorandom (PN) sequences will be shown to do almost as well. A ± 1 PN sequence of length $(2N+1)$ P has the property

$$\left[R_{2N+1}\right]_{ik} = \sum_{j=0}^{2N} d_{j-i} d_{j-k} = \begin{cases} 2N+1, & i = k \\ -1, & i \neq k \end{cases} \tag{9.83a}$$

i.e., its correlation with itself is, for any cyclical time shift, equals to -1. The inverse matrix R_{2N+1}^{-1} has elements

$$\left[R_{2N+1}^{-1}\right]_{ik} = \begin{cases} \dfrac{2}{(2N+1)+1}, & i = j \\ \dfrac{1}{(2N+1)+1}, & i \neq j \end{cases} \tag{9.83b}$$

Then from (9.80)

$$E||\mathbf{c}_n - \mathbf{h}_e||^2 = \sigma_v^2 \frac{2[2N+1]}{[2N+1]+1} . \tag{9.84}$$

For large $(2N+1)$, this is a factor of two worse than (9.82) for the orthogonal sequence, but it can be reduced by using more than $(2N+1)$ samples.

To converge the echo canceler in exactly $(2N+1)$ iterations we use the modified LMS algorithm

$$\mathbf{c}_{n+1} = \mathbf{c}_n + \beta\,(\mathbf{d}_n + \mathbf{1})\,e_n, \tag{9.85}$$

where $\mathbf{1}$ is a column vector whose elements are all equal to one, and β is a step size equal to $1/2N+1$. We will use the property of a *PN* sequence that

$$\mathbf{d}_n'\,\mathbf{1} = 1, \tag{9.86}$$

i.e., the sum of the elements of a *PN* sequence (which has almost, but not quite, an equal number of +1 and −1 elements) is one.

The proof that (9.85) converges in $(2N+1)$ steps is an inductive one suggested by Werner. First, recall (rewriting (9.32)) that the cancellation error is

$$e_n = d_n'\,(\mathbf{h}_e - \mathbf{c}_n) + \nu_n . \tag{9.87}$$

Assume an initial tap weight vector $\mathbf{c}_0 = \mathbf{0}$. Then from (9.85) and (9.87)

$$\mathbf{c}_1 = \beta(\mathbf{d}_0+\mathbf{1})\,(\mathbf{d}_0'\mathbf{h}_e+\nu_0) \tag{9.88a}$$

$$\begin{aligned}\mathbf{c}_2 &= \mathbf{c}_1 + \beta(\mathbf{d}_1+\mathbf{1})\,e_1 \\ &= \beta(\mathbf{d}_0+\mathbf{1})\,(\mathbf{d}_0'\mathbf{h}_e+\nu_0) + \beta(\mathbf{d}_1+\mathbf{1})\left[\mathbf{d}_1'(\mathbf{h}_e-\mathbf{c}_1)+\nu_1\right] \\ &= \beta\left\{(\mathbf{d}_0+\mathbf{1})\,(\mathbf{d}_0'\mathbf{h}_e+\nu_0) + (\mathbf{d}_1+\mathbf{1})\,(\mathbf{d}_1'\mathbf{h}_e+\nu_1)\right\} \\ &\quad - \beta^2\left\{(\mathbf{d}_1+\mathbf{1})\,\mathbf{d}_1'\,(\mathbf{d}_0+\mathbf{1})\,[\mathbf{d}_0'\mathbf{h}_e+\nu_0]\right\} .\end{aligned}$$

By property (9.83a), $\mathbf{d}_1\mathbf{d}_0' = -1$, since $\mathbf{d}_0$ is merely a cyclical shift, by one, of $\mathbf{d}_1$. By property (9.86), $\mathbf{d}_1'\mathbf{1} = 1$; thus

$$\mathbf{d}_1'\,(\mathbf{d}_0+\mathbf{1}) = 0,$$

implying that the β^2 term of $\mathbf{c}_2$ is zero, so that

$$\mathbf{c}_2 = \beta\left[(\mathbf{d}_0+\mathbf{1})(\mathbf{d}_0'h_e+\nu_0) + (\mathbf{d}_1+\mathbf{1})(\mathbf{d}_1'\mathbf{h}_e+\nu_1)\right] . \tag{9.88b}$$

Continuing to iterate in this way, we finally arrive at

$$\mathbf{c}_{2N+1} = \alpha \left[\sum_{j=0}^{2N} (\mathbf{d}_j + \mathbf{1})(\mathbf{d}_j' \mathbf{h}_e + \nu_j) \right] . \tag{9.88c}$$

But from (9.83a)

$$[R_{2N+1}]_{ik} = \left[\sum_{j=0}^{2N} \mathbf{d}_j \mathbf{d}_j' \right]_{ik} = \begin{cases} 2N+1, & i=k \\ -1 \quad , & i \neq k \end{cases} \tag{9.89a}$$

and from (9.86)

$$\left[\sum_{j=0}^{2N} \mathbf{1} \cdot \mathbf{d}_j' \right]_{ik} = 1 \quad \text{(a matrix of all ones)} .$$

Thus

$$\left[\sum_{j=0}^{2N} (\mathbf{d}_j + 1)\ \mathbf{d}_j' \right]_{ik} = \begin{cases} 2N+2, & i=k \\ 0 \quad , & i \neq k \end{cases} \tag{9.89b}$$

and with $\beta = 1/2N+1$, (9.88c) and (9.89b) yield

$$\mathbf{c}_{2N+1} = \mathbf{h}_e + \frac{1}{2N+1} \sum_{j=0}^{2N} (\mathbf{d}_j + \mathbf{1})\ \nu_0 .$$

Each element of $\mathbf{c}_{2N+1}$ has converged to the corresponding echo channel element plus a Gaussian random variable of mean zero and variance

$$E\left[\frac{1}{2N+1} \sum_{j=0}^{2N} (d_{jm}+1)\nu_j \right]^2 = \frac{1}{(2N+1)^2} \sum_{j=0}^{2N} E(d_{jm}+1)^2\ \sigma_\nu^2$$

$$= \frac{2\sigma_\nu^2}{2N+1}\ 1 ,$$

where d_{jm} is the ± 1 data random variable in the mth position of the jth data vector. The algorithm (9.85) has in fact converged in $(2N+1)$ steps, the size of the tap-weight vector, but with residual noise. Further adaptation, according to the stochastic adaptation algorithm (9.29) with a smaller step size β, can reduce the residual tap-weight fluctuation. Although fast startup by (9.85) has not yet been seen in practice because of other practical difficulties, such as restrictions on the length of the echo canceler, it is an excellent illustration of the opportunities for rapid convergence offered by special testing sequences.

It should be noted that there are other techniques for fast startup. Cioffi [27] describes a sounding technique using the discrete Fourier transform (DFT), and Ling and Long [17] propose white periodic complex training

sequences with orthogonal real and imaginary parts, correlated with the (real) echo to generate an echo channel estimate.

9.4 OTHER CANCELER STRUCTURES

The tapped delay line is not the only possible adaptive filter that could be utilized in an echo canceler. Although the FIR filter and the LMS adaptation algorithm are extremely robust, they are unable to handle nonlinear echo channel characteristics, and convergence is slower than that possible in some alternative structures. In this section, we will describe the lattice filter and memory canceler structures that can offer improved performance in some circumstances.

9.4.1 LATTICE FILTER CANCELER

An adaptive lattice filter is used for mean-square estimation of values of a correlated time sequence [22]. Its salient virtue is that of orthogonalizing successive driving inputs, which increases the rate of convergence. It is an obvious candidate for the adaptive filter of an echo canceler, although the advantages it might have for a line-signal-driven canceler, where successive Nyquist-interval samples of the driving waveform are correlated, are not evident for the data-driven cancelers we have been considering, where the driving sequence consists of uncorrelated data values. One can, of course, conceive of data-driven applications, such as natural language and facsimile data streams, where the data are in fact correlated. We will describe how the lattice filter canceler works.

Assume, as shown in Figure 9.26, a sampled-data echo cancellation system. A reference sequence $\{\ldots, s_{i-2}, s_{i-1}, s_i, \ldots\}$ drives a "black box" adaptive filter with output q_i which is subtracted from the incoming echo plus noise sampler r_i. The objective, as described by Honig [23], is to configure the black box to minimize the mean-square error $E[e_i^2]$.

Consider first predicting a reference sequence sample s_i as a linear combination of n past sequence samples. The error in the prediction is the nth-order forward prediction residual

$$e_f(i|n) = s_i - \mathbf{f}'(i|n)\mathbf{s}(i-1|n) \tag{9.90}$$

where

$$\mathbf{s}'(i|n) = \left[s_{i-n+1}, \ldots, s_i\right] \tag{9.91}$$

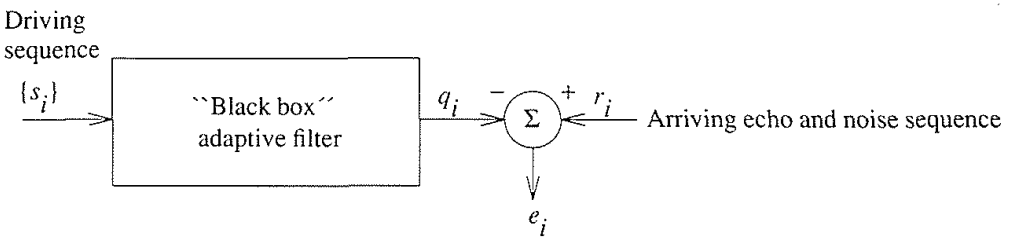

Fig. 9.26 Sampled-data echo cancellation with an adaptive "black box" filter.

is the vector of the most recent n samples of the reference sequence, and

$$\mathbf{f}'(i|n) = \left[f_{1|n}, \ldots, f_{n|n}\right] \tag{9.92}$$

is the vector of forward prediction coefficients. Similarly, one can predict a past sequence value s_{i-n} from n subsequent samples, yielding an nth-order backward prediction residual

$$e_b(i|n) = s_{i-n} - \mathbf{b}'(i|n)\mathbf{s}(i|n) , \tag{9.93}$$

where

$$\mathbf{b}'(i|n) = \left[b_{1|n}, \ldots, b_{n|n}\right] \tag{9.94}$$

is the vector of backward prediction coefficients. If the second-order statistics of the reference sequence are known, optimal values of the forward and backward prediction coefficients, minimizing $Ee_f^2(i|n)$ and $Ee_b^2(i|n)$ respectively, can be computed. It can be shown [22] that at any instant, the backward residuals are uncorrelated, i.e.,

$$E\left[e_b(i|m)e_b(i|n)\right] = \delta_{mn}\, E\left[e_b^2(i|n)\right] , \tag{9.95}$$

and that the optimum forward and backward prediction coefficients obey the recursive (order, not time) relationships

$$\begin{aligned} e_f(i|n) &= e_f(i|n-1) - K_n(i)e_b(i-1, n-1) \\ e_b(i|n) &= e_b(i-1|n-1) - K_n(i)e_f(i, n-1) , \end{aligned} \tag{9.96}$$

where $1 \le n \le N$ = the order of the filter, and the "parcor" (partial correlation) coefficients are defined as

$$K_n(i) \triangleq E\left[e_f(i|n-1)e_b(i-1|n-1)\right] \Big/ E\left[e_f^2(i|n-1)\right] . \tag{9.97}$$

The recursion relationships (9.96) are graphically represented by the lattice of Figure 9.27. The lattice begins (at the left) by estimating the residuals $e_f(i|1)$

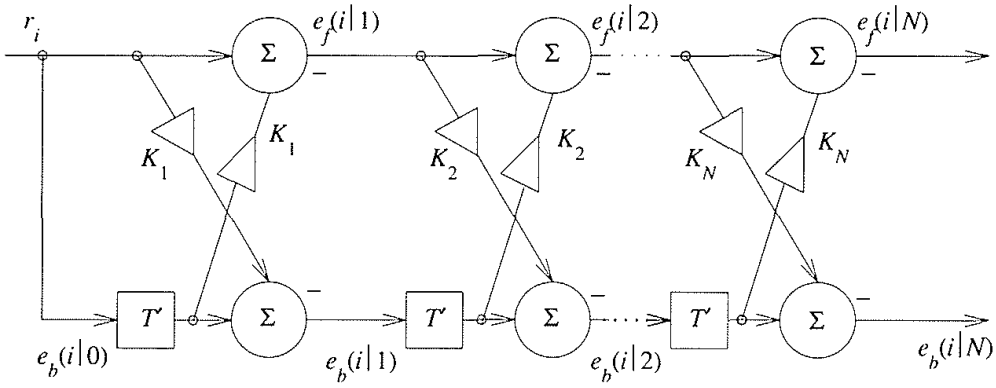

Fig. 9.27 Lattice structure for order-recursive generation of reference sequence prediction coefficients.

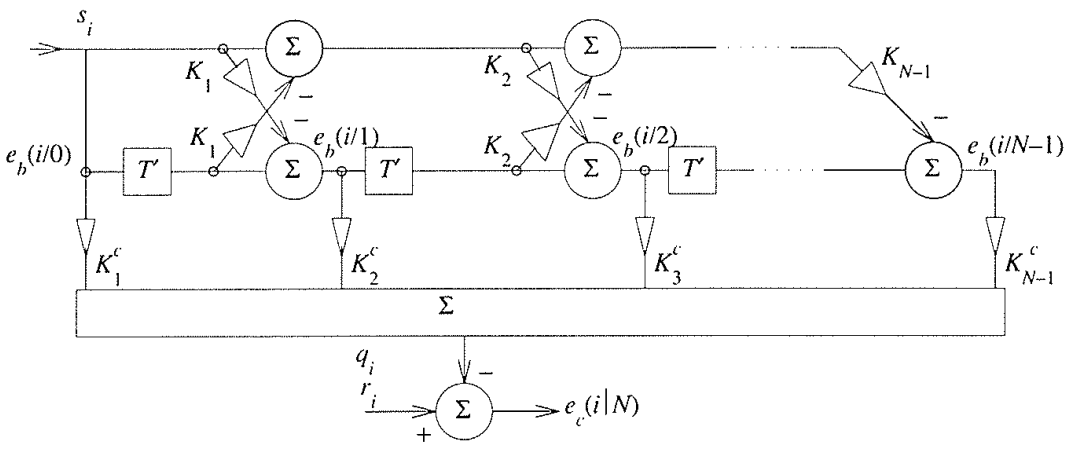

Fig. 9.28 Lattice echo canceler.

and $e_b(i|1)$ from the current (r_i) and most recent past (r_{i-1}) received samples.

The structure of Figure 9.27 yields prediction residuals for a driving signal consisting of one scalar value, s_i, at the ith iteration. For the echo cancellation application, however, the echo estimate q_i at the ith iteration, which in the tapped delay line structure is formed from the (possibly correlated) N-dimensional input sample vector,

$$\mathbf{s}'(i|N) = \left[s_{i-N+1}, \ldots, s_i\right], \tag{9.98}$$

is generated as a linear combination of the (uncorrelated) backward prediction residuals $[e_b(i|0), \ldots, e_b(i|N-1)]$. That is,

$$q_i = \sum_{n=0}^{N-1} K_{n+1}^c \, e_b(i|n) \, . \tag{9.99}$$

Thus, as shown in Figure 9.28, the post-cancellation error is

$$e_i = r_i - q_i = r_i - \sum_{n=0}^{N-1} K_{n+1}^c \, e_b(i|n) \, . \tag{9.100}$$

The coefficients $\{K_n^c\}$ which minimize $E\left[e_i^2\right]$ are readily derived (Exercise 9.5), yielding

$$\begin{aligned} K_n^c &= E\left[r_i e_b(i|n-1)\right] \Big/ E\left[e_b^2(i|n-1)\right] \\ &= E\left[e_c(i|n-1) e_b(i|n-1)\right] \Big/ E\left[e_b^2(i|n-1)\right] \, , \end{aligned} \tag{9.101}$$

where $e_c(i|n-1)$ has been defined as an $(n-1)$th-order filter residual of the cancellation error e_i, such that $e_c(i|N) = e_i$. Note that the coefficients are the normalized correlation of the (output) error and the voltage at the corresponding

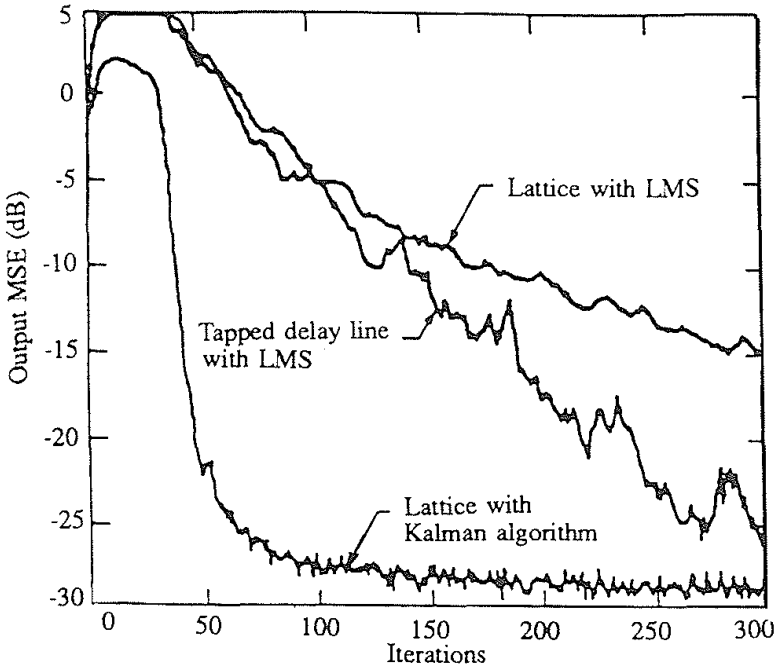

Fig. 9.29 Relative performance of lattice and tapped delay line cancelers with $N = 30$ taps, on an echo channel with exponential impulse response ($r_i = 0.96^i$) and SNR = 40 dB. The stochastic adaptation (LMS) algorithem was used in these simulations. Operation of the lattice with the Kalman adaptation algorithm is also shown. From Honig [23].

weight. The residual obeys, from (9.100), the recursion

$$e_c(i|n) = e_c(i|n-1) - K_n^c e_b(i|n-1) . \qquad (9.102)$$

As we have noted, the performance of the lattice structure for an uncorrelated driving sequence is not superior to that of the tapped delay line, as shown in Figure 9.29. In fact it is worse, when adapted via the LMS algorithm, because of statistical fluctuations of the forward and backward prediction coefficients, which, in the case of an uncorrelated driving sequence, should be equal to zero. It has, however, been shown to be superior in cases where the driving sequence was correlated [23,24], as well as when "fast" adaptation algorithms, such as the Kalman algorithm described in Chapter 8 for channel equalization, are applied to echo cancellation (see Figure 9.29). Note that Figure 9.29 shows the ability of the Kalman algorithm to significantly improve convergence relative to the LMS algorithm, even when the inputs to the canceler are uncorrelated. As with equalizers, the Kalman and fast Kalman algorithms can be applied to both tapped delay line and lattice structures.

9.4.2 MEMORY COMPENSATION STRUCTURES

The transversal filter and lattice echo cancelers described so far, with multiple tap weights adapted to minimize mean-square error, have several disadvan-

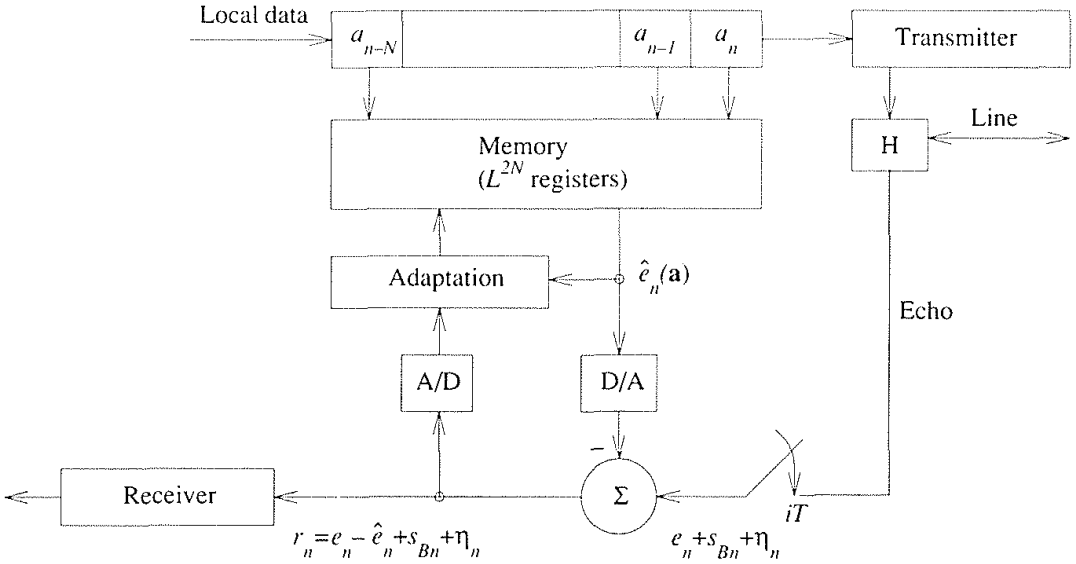

Fig. 9.30 Principle of memory echo canceler.

tages. Even when data-driven, the updating and filtering operations are computationally intensive, requiring high-speed logic. But most significantly, the echo canceler cannot replicate a nonlinear echo channel.

If the number L of pulse levels is small, and the echo channel memory, denoted as N symbol intervals, is not too long, there is a very simple and elegant way to realize a nonlinear canceler [25]. It is based on the observation that e_n (Figure 9.30), the echo sample at the receiver input at the nth symbol-interval sampling time nT, is completely determined by the N most recent local data values, denoted as the vector $\mathbf{a}(n)$, and the echo channel.

Let $\mathbf{a}_k$ denote the kth of the L^N values of this data vector. As Figure 9.30 illustrates, a memory simply stores all L^N possible values of $\hat{e}_n$. The contents of the register addressed by the current value of the data vector $\mathbf{a}(n)$ is simply read out as the echo estimate $\hat{e}_n$ and fed to the subtracter.

The memory echo canceler works only under special circumstances, fortunately the case for most digital subscriber lines (but not most dialed telephone circuits):

1. The echo channel changes only very slowly.
2. The clocks of the transmitters at the two ends of the subscriber line are locked together, so that the sampling times $nT + t_0$, with the sampling epoch t_0 chosen for best reception of the distant signal, are at a fixed delay t_0' from the transitions in the local data train $\{a_i\}$.

Condition (1) assures that the weak tracking capability of the memory canceler is not a problem, and condition (2) guarantees that there is no drift in the

sampling time with respect to the local data train. A drift in the sampling time would require a change in the stored value $\hat{e}_n$ corresponding to a particular data vector **a**.

Given these conditions, a simple stochastic adaptation algorithm is one that minimizes the power

$$\left[r_n\right]^2 = \left[e_n - \hat{e}_n(\mathbf{a}) + s_{Bn} + \eta_n\right]^2 \tag{9.103}$$

of each symbol-interval sample of the post-cancellation error signal, where a particular N-element reference data sequence **a** happens to be in the shift register of Figure 9.30 at time nT. The effect, over many data symbols, is to minimize the average error-signal power; since the far-end signal and noise are independent of e_n and $\hat{e}_n$, this means that $\hat{e}_n \rightarrow e_n$.

The vector **a** addresses a particular location in the memory, where an echo estimate $\hat{e}_n(\mathbf{a})$ is stored at time nT, and it is this particular stored value, and it only, which is adapted when **a** is the reference input. No other stored data are adapted. Adaptation is according to a negative gradient algorithm:

$$\begin{aligned}\hat{e}_{n+1}(\mathbf{a}) &= \hat{e}_n(\mathbf{a}) - (\alpha/2)\partial r_n^2/\partial \hat{e}_n(\mathbf{a}) \\ &= \hat{e}_n(\mathbf{a}) + \alpha r_n \ .\end{aligned} \tag{9.104}$$

The value of α is, as usual, a compromise between fast convergence and small residual error after convergence. If $s_{Bn} + \nu_n$ in Figure 9.30 were zero, making $r_n = e_n - \hat{e}_n$, α could be made equal to one and the correction would make the echo estimate equal to the echo.

The complexity of the canceler of Figure 9.30 can be reduced by using a sign algorithm, allowing removal of the A/D converter and resulting in the adaptation algorithm

$$\hat{e}_{n+1}(\mathbf{a}) = \hat{e}_n(\mathbf{a}) + \Delta \ \mathrm{sgn}(r_n + \xi_n) \ , \tag{9.105}$$

where ξ_n is a uniformly distributed "dithering" noise, over a range comparable to the amplitude range of r_n, which reduces quantization error on the average, and Δ is the quantization step size of the memory registers, normalized by the RMS value of $r_n + \xi_n$. As a penalty for its computational simplicity, the sign algorithm tracks much more slowly than (9.104).

9.5 PASSBAND CONSIDERATIONS

We have so far presumed a baseband data communication system and examined echo cancelers for attenuation of baseband echos. But for many echo cancellation requirements, the echo is a passband modulated signal, as suggested in Figure 9.31. If one uses a data-driven echo canceler, some means must be found to synthesize a passband echo from a baseband data stream. There are several realization alternatives, both baseband and passband, described in the

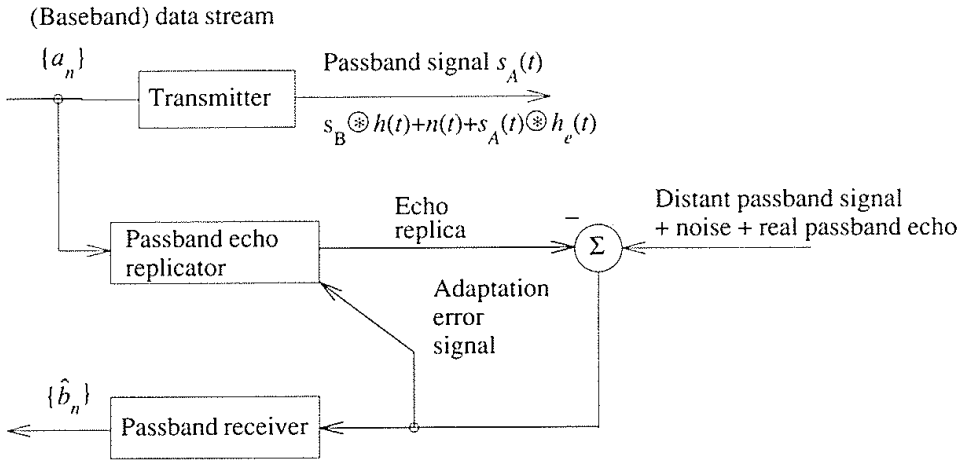

Fig. 9.31 Data-driven echo cancellation for passband echo.

following two subsections. There are also the transmission impairments of phase jitter and frequency offset on the distant echo, for which compensation can be arranged, as described in Section 9.5.3.

9.5.1 COMPLEX NOTATION FORMULATION

Referring to Figure 9.32, the complex transmitted signal is

$$\tilde{s}_A(t) = \sum_n \tilde{d}_n \, p(t-nT) \, e^{j2\pi f_c t}, \tag{9.106}$$

where the $\{\tilde{d}_n\}$ are, as in Section 5.2.1 of Chapter 5, the complex data levels corresponding to points in a two-dimensional signal constellation. The echo

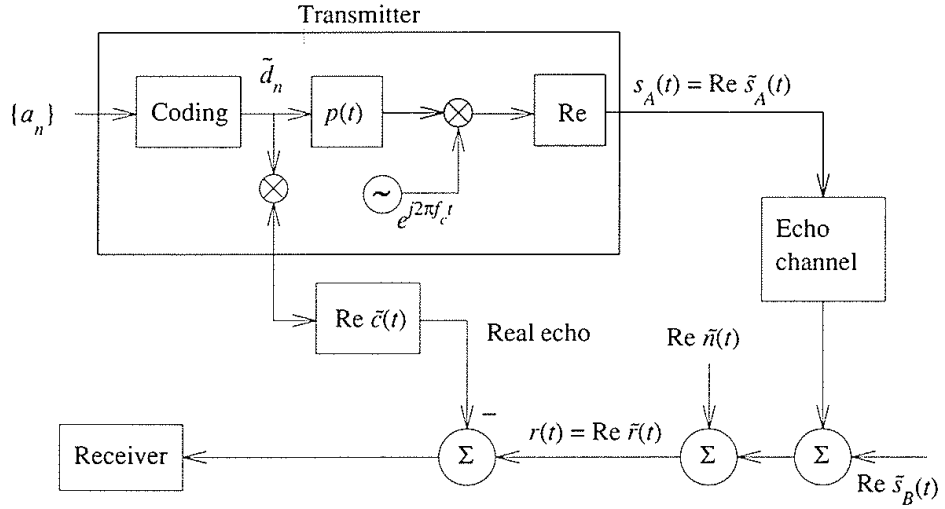

Fig. 9.32 Complex terminology. The echo characteristic $h_e(t) = \text{Re}\, \tilde{h}_e(t)$ is composed of $p(t)$ and the echo channel.

channel satisfies the relationships

$$h_e(t) = R_e\ \tilde{h}_e(t)$$

and

$$\tilde{h}_e(t) = \tilde{h}_{eBB}(t)\ e^{j2\pi f_c t}, \tag{9.107}$$

where $\tilde{h}_e(t)$ is the complex analytic echo channel and $\tilde{h}_{eBB}$ is the equivalent complex baseband echo channel. We assume that $h_e(t)$ includes the transmitter pulse filter $p(t)$. Thus the received signal just before the canceler of Figure 6.32 is

$$r(t) = \text{Re}\ \tilde{r}(t) = \text{Re}\left[\sum_n \tilde{d}_n\ \tilde{h}_e[t-nT]\ e^{j2\pi f_c t} + \tilde{n}(t) + \tilde{s}_B(t)*\tilde{h}(t)\right], \tag{9.108}$$

where $\tilde{n}(t)$ is the complex analytic noise, $\tilde{s}_B(t)$ is the complex analytic distant signal, and $\tilde{h}(t)$ is the complex analytic transmission channel from the distant transmitter.

The echo canceler and receiver will ordinarily be implemented as digital signal processors operating at a sampling rate at least as large as the Nyquist rate. Thus the canceler will deal with received signal samples

$$r(nT') = \text{Re}\left[\sum_n \tilde{d}_n \tilde{h}_e(nT'-nT)e^{j2\pi f_c nT'} + \tilde{n}(nT') + \tilde{s}_B(t)*\tilde{h}(t)\,\Big|_{nT'}\right]. \tag{9.109}$$

The canceler will generate echo replica samples at these same time instants nT', as described in Section 9.3.6, but not all samples may have to be generated.

The signal processing in the echo canceler can also be represented in complex notation. The canceler is attempting to create a replica of $\tilde{h}_e(t)$ or its real part. We will let $\tilde{\mathbf{c}}_i(n)$ denote the (complex) tap weight vector, at time $nT+iT'$, of the ith symbol-interval subcancelers. Similarly, $\tilde{e}_i(n)$ denotes the complex error after subtraction of the echo replica. If $A = E\ a_n^2 = Eb_n^2$, then

$$E|\tilde{d}_n|^2 = 2A, \tag{9.110}$$

and formula (9.38) for the mean-square error becomes [16]

$$E|\tilde{e}_i(n)|^2 = [1-2\beta A+2\beta^2(2N+1)A^2]\ E|\tilde{e}_i(0)|^2 + \frac{1-(1-2\beta A+2\beta^2(2N+1)A^2)^2}{1-(1+2\alpha A+2\alpha^2(2N+1)A^2)} \cdot 2\beta A\sigma^2 . \tag{9.111}$$

9.5.2 COMPLEX CANCELER ALTERNATIVES

As we shall see, the signal processing in the echo canceler can also be presented in complex analytic notation. The canceler is attempting to create a

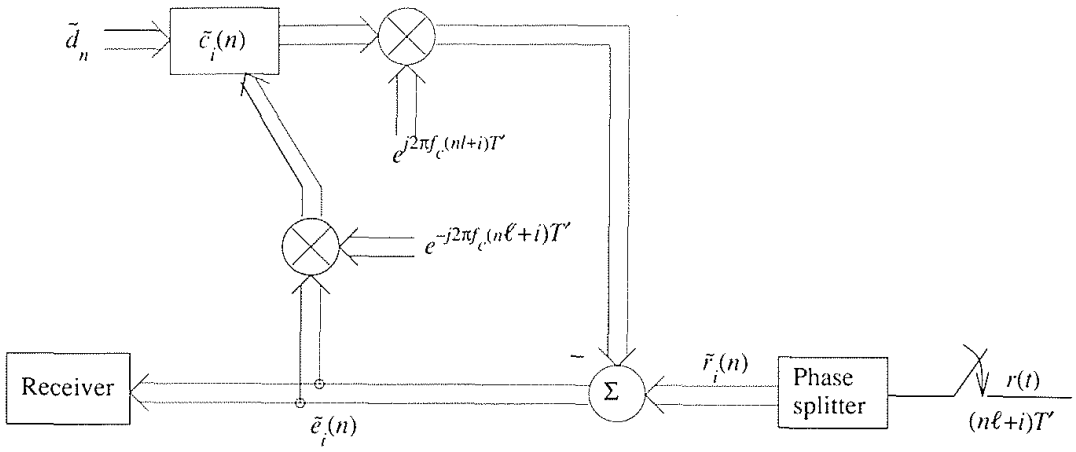

Fig. 9.33 A complex canceler with baseband adaptation.

replica of $\tilde{h}_e(t)$, and it can do this in separate steps of adaptive filtering and translation to passband, as described in this section, or, under certain conditions, by direct inband signal generation.

The various configurations differ in whether adaptive filtering is done in baseband or passband, in the complexity of implementation, and in the speed of convergence. A comparison of some of the alternatives is made in the paper by Im et al. [26].

Figure 9.33 pictures one of the alternatives, a complex adaptive baseband filter, followed by a multiplication by $\exp[j2\pi f_c nT']$ that does the translation to passband, followed by a complex subtracter [19] The algorithm is described below, but the convergence analyses, similar to the real baseband version described in Section 9.3.6, are not reproduced here.

The subtraction of the echo replica from the complex analytic received signal requires generation of the complex analytic received signal in a phase splitter that includes a Hilbert filter (phase splitter), as illustrated in Figure 5.13 of Chapter 5. However, no one has been able to build a Hilbert filter, of acceptable delay and complexity, that is accurate enough for 60 dB ERLE in the complex subtracter. For this reason, and complexity considerations, designers have looked for modification of this basic fractionally-spaced design. The complexity has already been characterized in Section 9.3.6 as $8(2N+1)/T'$ real multiplications per second. All of these multiplications are, however, relatively simple, using as factors values of $\{d_n\}$, which take on only a few distinct values.

With complex processing (9.60) and (9.63) for filtering and updating respectively take on the forms

$$\left.\begin{aligned} \tilde{y}_{n\ell+i} &= \left[\tilde{\mathbf{c}}_i'(n)\tilde{\mathbf{d}}(n)\right] e^{j2\pi f_c(n\ell+i)T'} \\ \tilde{\mathbf{c}}_i(n+1) &= \tilde{\mathbf{c}}_i(n) + \beta\left[\tilde{e}_i(n)e^{-j\pi f_c(n\ell+i)T'}\right]\tilde{\mathbf{d}}(n) \end{aligned}\right\} i = 0,\ldots,\ell-1 . \quad (9.112)$$

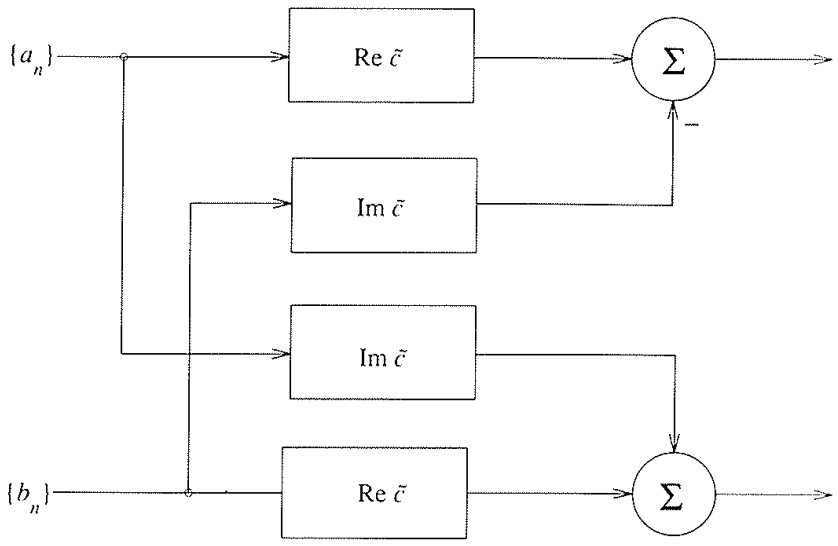

Fig. 9.34 The cross-coupled (full complex) filter.

Where, as in (9.56), $\ell = T/T'$, n is the time index in units of the symbol interval T, and i is the index of a particular symbol-interval subcancelers. The complex passband error sample $\tilde{e}_i(n)$, which is the error sample at time $t = (n\ell + i)T'$, is translated to baseband by the exponential with negative exponent.

To get around the phase splitter problem, the algorithm can be modified, at some cost in rate of convergence, by doing the subtraction in real variables and using the real error to drive the adaptation algorithm

$$\tilde{\mathbf{c}}_i(n+1) = \tilde{\mathbf{c}}_i(n) + \beta\, \mathrm{Re}\left[\tilde{e}_i(n)\right] e^{-j2\pi f_c (n\ell + i)T'} \tilde{\mathbf{d}}(n) . \quad (9.113)$$

It should be noted that (9.111) describes a *cross-coupled* structure. The product $\tilde{\mathbf{c}}_i'(n)\tilde{\mathbf{d}}(n)$ is, dropping the indices for convenience and recalling that a data symbol has real and imaginary components a and b respectively,

$$\begin{aligned}\tilde{\mathbf{c}}'\tilde{\mathbf{d}} &= \left[\mathrm{Re}(\tilde{\mathbf{c}}) + i\ \mathrm{Im}(\tilde{\mathbf{c}})\right]' \left[\mathbf{a} + j\mathbf{b}\right] \\ &= \mathrm{Re}(\tilde{\mathbf{c}})'\,\mathbf{a} - \mathrm{Im}(\tilde{\mathbf{c}})'\mathbf{b} + j\left[\mathrm{Re}(\tilde{\mathbf{c}})'\mathbf{b} + \mathrm{Im}(\tilde{\mathbf{c}})'\mathbf{a}\right] . \quad (9.114)\end{aligned}$$

These four inner products are indicated in Figure 9.34.

Rather than generate a filter characteristic first and modulate to passband second, an echo canceler can modulate the data to passband first and adapt a *passband* filter second, as shown in Figure 9.35. The algorithm is expressed as

$$\begin{aligned}\tilde{y}_{n\ell+i} &= \tilde{\omega}_i'(n)\left[\tilde{\mathbf{d}}(n)\ e^{j2\pi f_c (n\ell+i)T'}\right] \\ \tilde{\omega}_i(n+1) &= \tilde{\omega}_i(n) + \beta\tilde{e}_i(n)\left[\tilde{\mathbf{d}}_{(n)}\ e^{j2\pi f_c (n\ell+i)T'}\right], \quad (9.115)\end{aligned}$$

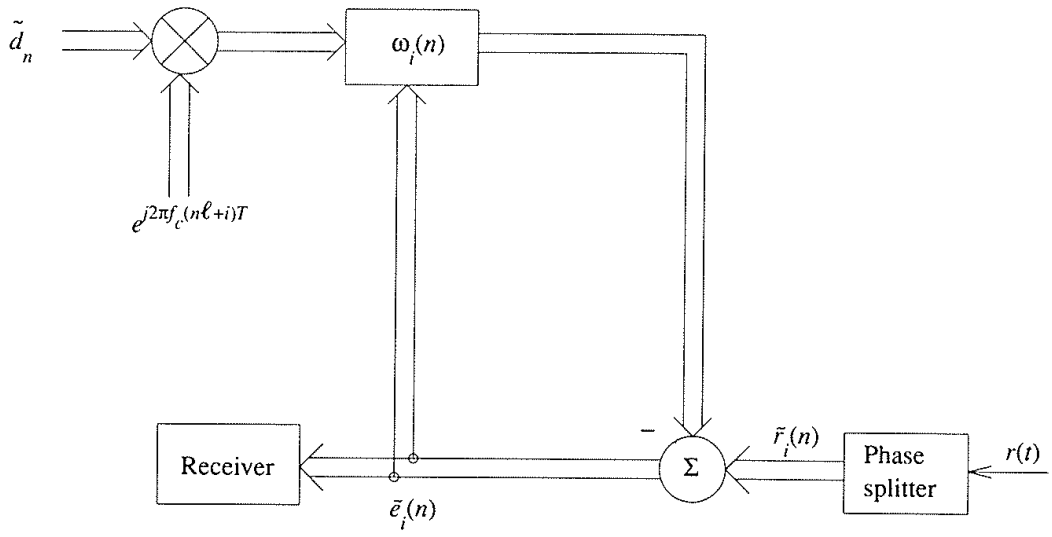

Fig. 9.35 Complex echo canceler with passband adaptive filtering.

where $\tilde{\omega}$ represents the passband filter tap weights. If $f_c T'$ equals a rational number, there are only a finite number of different phase rotations of $\tilde{\mathbf{d}}(n)$, analogous to what was described earlier as an option for the canceler with a baseband filter. Here, however, the cross-coupled complex filter can be reduced to a pair of real filters, since that is all that is needed to produce the real echo replica. This is shown in Figure 9.36. Cancellation with real signals avoids the phase-splitter problem alluded to earlier. The cost, of course, is in rate of convergence.

This non-cross-coupled structure is sometimes used for near-echo cancellation, with the cross-coupled structure reserved for the more difficult distant echo, which may suffer phase perturbations. The arrangement is suggested in Figure 9.37. With much of the near echo canceled, the ERLE expected of the far-echo canceler is modest and a phase splitter becomes practical.

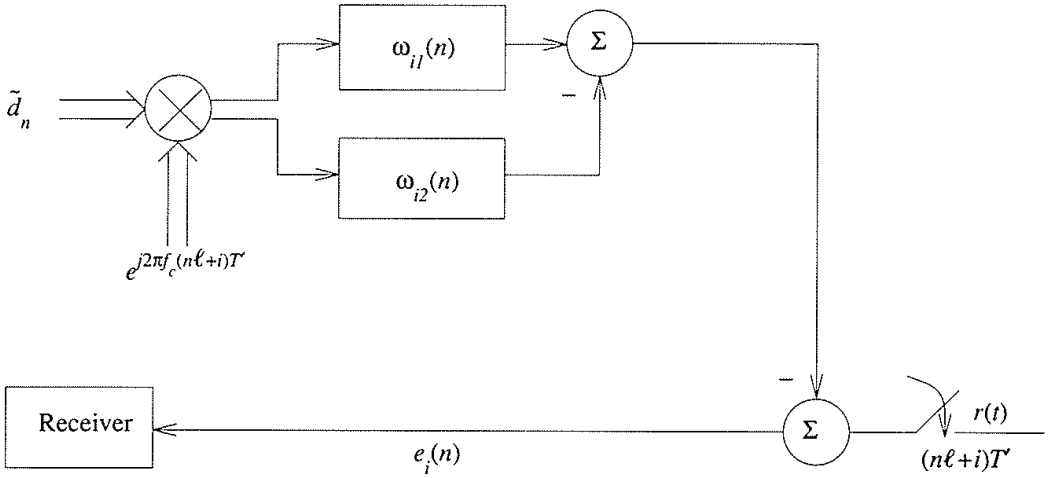

Fig. 9.36 Complex echo canceler with simplified passband adaptive filtering for real output only.

9.5.3 PHASE JITTER/FREQUENCY OFFSET COMPENSATION

The distant echo, having in some cases transversed FDM carrier systems, may arrive back at the source station with phase perturbation introduced in carrier systems, as explained in Chapter 1. A transversal filter operating an echo replica can, theoretically, generate the phase notations caused by phase jitter frequency offset, but in practice it cannot adapt fast enough to track most phase perturbations.

The situation is very similar to phase tracking on the forward channel, described in detail in Chapter 6. If (using complex notation) a phase perturbation represented by $e^{j\theta(t)}$ is present in the echo channel following the linear distortion, as illustrated in Figure 9.38, it can be partly canceled by a phase factor $e^{-j\hat{\theta}(t)}$. To achieve this, a first-order phase tracking loop can be derived as follows. The complex error following echo cancellation is

$$\tilde{e}_i(n) = \tilde{r}_i(n) - e^{\hat{\theta}_i(n)}\, \tilde{\mathbf{c}}_i(n)'\tilde{\mathbf{d}}(n) \,. \tag{9.116}$$

The gradient adaptation algorithm is

$$\hat{\theta}_i(n) = \hat{\theta}_i(n-1) - \frac{\lambda}{2}\,\frac{\partial|\tilde{e}_i(n)|^2}{\partial\theta} \,, \tag{9.117}$$

and since

$$\frac{\partial|\tilde{e}_i(n)|^2}{\partial\theta} = 2\ \mathrm{Im}\left[\tilde{e}_i(n)e^{-j\hat{\theta}_i(n)}\ \tilde{\mathbf{c}}_i^*(n)'\tilde{\mathbf{d}}^*(n)\right] \,, \tag{9.118}$$

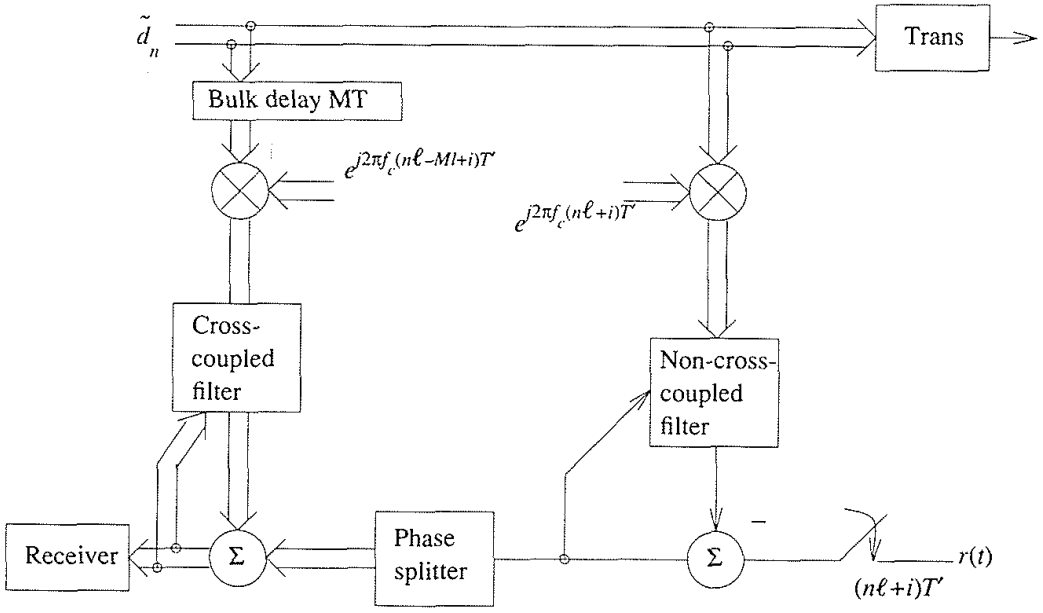

Fig. 9.37 Echo canceler with cross-coupled filter for distant echo and non-cross-coupled filter for near echoes.

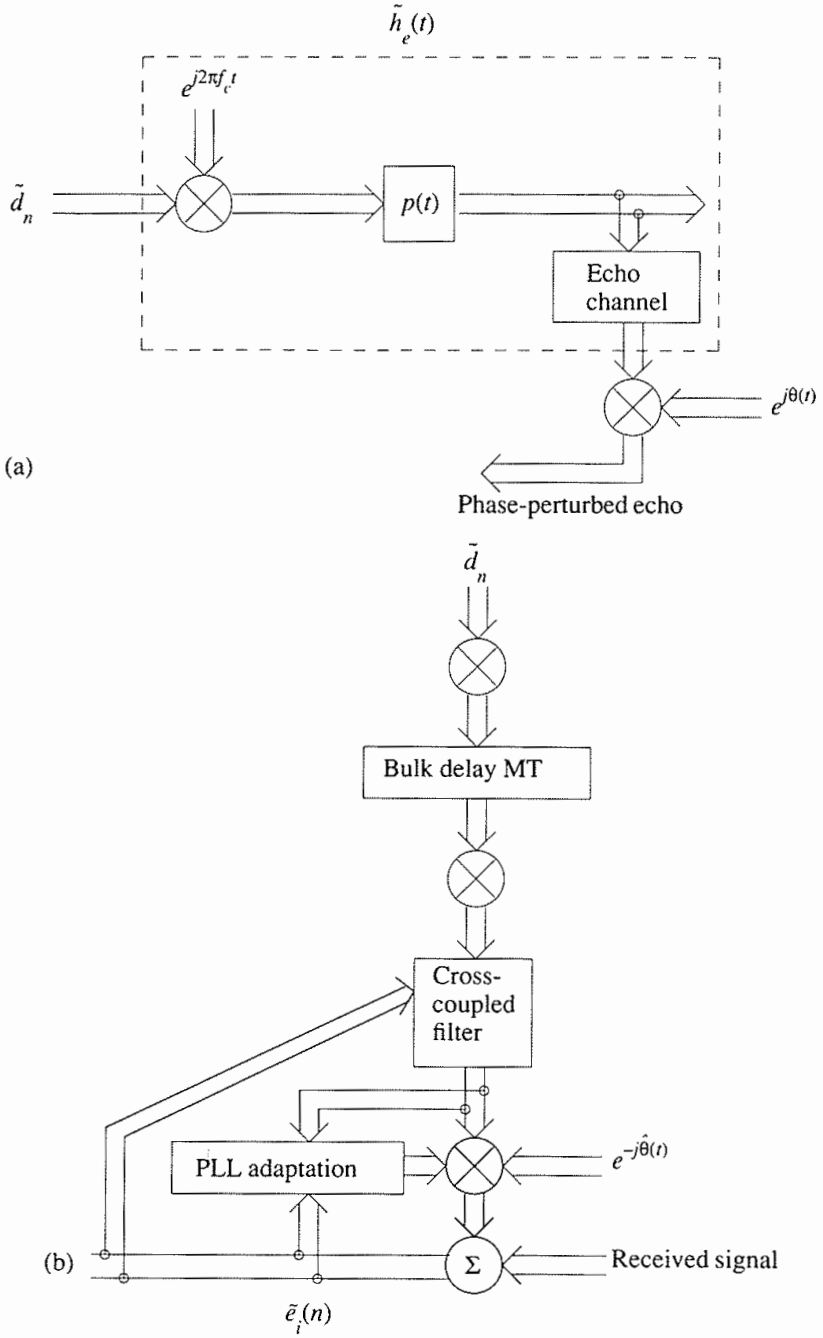

Fig. 9.38 Phase tracking for distant echo. (a) Introduction of phase perturbation $\theta(t)$ in echo channel. (b) Phase-locked tracking loop.

we have

$$\hat{\theta}_i(n) = \hat{\theta}_i(n-1) + \lambda \operatorname{Im}\left[\tilde{e}_i(n)\, e^{-j\hat{\theta}_i(n)}\, \tilde{\mathbf{c}}_i^*(n)'\, \tilde{\mathbf{d}}^*(n)\right]. \quad (9.119)$$

Further analysis similar to that in Chapter 6 shows that, in the absence of linear

distortion and noise,

$$E\left[\tilde{e}_i(n)\, e^{-j\hat{\theta}_i(n)}\ \tilde{\mathbf{c}}_i^*(n)'\,\tilde{\mathbf{d}}^*(n)\right] \sim \sin\left[\theta_i(n)-\hat{\theta}_i(n)\right], \qquad (9.120)$$

so that (9.119) does indeed approximate a first-order phase-locked loop.

The phase perturbation is often largely a linearly increasing phase

$$\theta(t) = 2\pi f_{off} t, \qquad (9.121)$$

where f_{off} is the *frequency offset*. The frequency offset is rarely greater than 1 Hz. A second-order phase-locked loop might be considered, requiring minimum tracking bandwidth, not really true because of the need to track under double-talking conditions so that the step size γ in (9.119) has to be made small. In practice, even for small frequency offset, it is found that a second-order loop is required (see Harman, Wang, and Werner, [28]) but a first-order loop is adequate, since the frequency offset is small enough and may be combined with phase jitter.

9.5.4 PERFORMANCE WITHOUT AND WITH PHASE TRACKING

Wang and Werner [28,30] derive expressions for the echo return loss enhancement in non-cross-coupled and cross-coupled symbol interval echo cancelers perturbed by frequency offset, without any phase tracking. In the first case, the ERLE is

$$ERLE = 10\log\left[\frac{1-\beta A}{1-\beta(2N+1)A}\cdot\frac{\Delta^2}{\beta^2 A+(1-\beta A)\Delta^2}\right], \qquad (9.122a)$$

where $\Delta = 2\pi f_{OFF} T$. In the second case,

$$ERLE = -10\log\left[\frac{1-\beta A}{1-\beta(2N+1)A}\cdot\frac{\Delta^2}{4\beta^2 A^2+(1-2\beta A)\Delta^2}\right]. \qquad (9.122b)$$

For practical values of the parameters, the cross-coupled structure performs about 6 dB better.

REFERENCES

[1] A. Brosio, U. DeJulio, V. Lazzari, R. Ravaglia, and A. Topanelli, "A comparison of digital subscriber line transmission systems employing different line codes," *IEEE Trans. on Communications*, Vol. COM-29, No. 11, pp. 1581–1588, November 1981.

[2] J. Bingham, *Theory and Practice of Modem Design*, Wiley, 1988.

[3] S. Yoneda and Y. Fukui, "Suppression of impedance fluctuations in hybrid couplers," *IEEE Trans. on Communications*, Vol. COM-27, No. 1, pp. 102–105, January 1984.

[4] S. B. Weinstein, "Echo cancellation in the telephone network," *IEEE Communications Magazine*, Vol. 15, No. 1, pp. 9–15, January 1987.

[5] F. K. Becker, and H. R. Rudin, "Application of automatic transversal filters to the problem of echo suppression," *Bell System Tech. J.*, Vol. 45, No. 12, pp. 1947–1850, December 1966.

[6] M. M. Sondhi, and A. J. Presti, "A self-adaptive echo canceler," *Bell System Tech. J.*, Vol. 45, No. 10, pp. 1851–1854, December 1966.

[7] M. M. Sondhi, "An adaptive echo canceler," *Bell System Tech. J.*, Vol. 46, No. 3, pp. 497–511, March 1967.

[8] D. L. Duttweiler, "A twelve-channel digital echo canceler," *IEEE Trans. on Communications*, Vol. COM-26, No. 5, pp. 647–653, May 1978.

[9] D. G. Messerschmitt, "Echo cancellation in speech and data transmission," *IEEE Journal on Selected Areas in Communications*, SAC-2, No. 2, March 1984.

[10] N. S. Lin and C. P. J. Tzeng, "Full-duplex data transmission over local loops," *IEEE Communications Magazine*, Vol. 26, No. 2, pp. 31–47, February 1988.

[11] D. G. Messerschmitt, "Design issues in the ISDN U-interface transceiver," *IEEE Journal on Selected Areas in Communications*, Vol. SAC-4, pp. 1281–1293, November 1986.

[12] M. Honig, K. Steiglitz, and B. Goppuath, "Multichannel signal processing for data communications in the presence of crosstalk," IEEE Trans. on Communications, Vol. 38, No. 4, pp. 551–558, April 1990.

[13] V. G. Koll and S. B. Weinstein, "Simultaneous two-way data transmission over a two-wire circuit," *IEEE Trans. on Communications*, Vol. COM-21, No. 2, pp. 143–147, February 1973.

[14] D. D. Falconer and K. H. Mueller, "Adaptive echo cancellation/AGC structures for two-wire full-duplex transmission on two-wire circuits," *Bell System Tech. J.*, Vol. 58, pp. 1593–1616, September 1979.

[15] K. H. Mueller, "A new digital echo canceler for two-wire full-duplex data transmission," *IEEE Trans. on Communications*, Vol. COM-24, No. 9, pp. 956–967, September 1976.

[16] J. J. Werner, "An echo-cancellation-based 4800 bit/s full-duplex DDD

modem," *IEEE Journal on Selected Areas in Communications*, Vol. SAC-2, No. 5, pp. 722–730, September 1984.

[17] F. Ling and G. Long, "Correlation-based fast training of data-driven Nyquist in-band echo cancelers," *Proceedings ICC '90*, Atlanta, pp. 1280–1284, April 1990.

[18] N. A. M. Verhoeckx, H. C. Van den Elzen, F. A. M. Snijders, and P. J. Van Gerwen, "Digital echo cancellation for baseband data transmission," *IEEE Trans. on Acoustics, Speech, and Signal Processing*, Vol. ASSP-27, No. 6, December 1979.

[19] S. B. Weinstein, "A passband data-driven echo canceler for full-duplex transmission on two-wire circuits," *IEEE Trans. on Communications*, Vol. COM-26, No. 7, pp. 654–666, July 1977.

[20] R. D. Gitlin and S. B. Weinstein, "The effects of large interference on the tracking capability of digitally echo cancelers," *IEEE Trans. on Communications*, pp. 833–839, June 1978.

[21] D. D. Falconer, "Adaptive reference echo cancellation," *IEEE Trans. on Communications*, Vol. COM-30, No. 9, pp. 2083–2094, September 1982.

[22] B. Friedlander, "Lattice filters for adaptive processing," *Proc. IEEE*, Vol. 70, pp. 829–867, August 1982.

[23] M. Honig, "Echo cancellation of voiceband data signals using recursive least squares and stochastic gradient algorithms," *IEEE Trans. on Communications*, Vol. COM-33, No. 1, pp. 65–73, January 1985.

[24] E. H. Satarius and J. D. Pack, "Application of least squares lattice algorithms to adaptive equalization," *IEEE Trans. on Communications*, Vol. COM-29, pp. 136–142, February 1981.

[25] N. Holte and S. Stueflotten, "A new digital echo canceler for two-wire subscriber lines," *IEEE Trans. on Communications*, Vol. COM-29, No. 11, pp. 1573–1581, November 1986.

[26] G. H. Im, L. K. Un, and J. C. Lee, "Performance of a class of adaptive data-driven echo cancelers," *IEEE Trans. on Communications*, Vol. COM-37, No. 12, pp. 1254–1263, December 1989.

[27] J. Cioffi, "A fast echo canceler initialization method for the CCITT V.32 modem," *Proc. Globecom '87*, Tokyo, pp. 1950–1954, November 1987.

[28] D. Harman, J. D. Wang, and J. J. Werner, "Frequence Offset Compensation Techniques for Echo-Cancellation Based Modems," *Conference Record Globecom '87*, Tokyo, Japan.

[29] J. J. Werner, "Effects of channel impairments on the performance of an in-band data-driven echo canceler," *AT&T Tech. J.*, Vol. 64, No. 31, pp. 91–113, January 1985.

[30] J. D. Wang, and J. J. Werner, "Performance analysis of an echo-cancellation arrangement that compensates for frequency offset in the far echo," *IEEE Trans. on Communications*, Vol. 36, No. 3, pp. 364–372, March 1988.

[31] J. Salz, "On the start-up problem in digital echo canceler," *Bell System Tech. J.*, Vol. 60, No. 10, pp. 2345–2358, July-August 1983.

EXERCISES

9.1: A time-compression multiplexing system is to provide continuous full-duplex data communication at 100 kbps in each direction. Assume that the one-way, end-to-end propagation time is 10 ms, and a station does not start a transmission burst until it has observed the end of the transmission burst from the other direction

(a) What value of the buffer capacity yields the minimum transmission burst rate? What is that minimum burst rate? What burst rate yields the minimum buffer size? What is that size? [Hint: These are extreme cases.]

(b) For a realistic buffer capacity of 10,000 bits, what is the burst transmission rate? The end-to-end transmission delay (including buffer delay)?

(c) For this burst transmission rate, and if four-level baseband PAM with 50% rolloff is used for the line signal in each direction, what is the required bandwidth?

9.2: Prove that for a linear echo channel $h_e(t)$, the echo canceler incorporating an infinite-length transversal filter with taps spaced at $T' < 1/2f_{\max}$, where $f_{\max}$ is the highest frequency component of the bandlimited echo signal, cancels perfectly, and has tap weights equal to samples of the echo channel.

9.3: Starting from the relationship

$$E\, e_n^2 = A\, E\{\xi_n'\, \xi_n\} + \sigma^2 \,, \tag{9.35}$$

$$e_{n+1} = \xi_{n+1}'\, \mathbf{d}(n+1) + \nu_{n+1} \,, \tag{9.36}$$

where ξ_n is the tap-weight error vector, ν_n is noise uncorrelated with the data, and $\sigma^2 E\, \nu_n^2$, and $(2N+1)$ is the number of taps, show that

$$\left[1 - 2\beta A + \beta^2(2N+1)A^2\right] E\{e_n^2\} + 2\beta A\, \sigma^2 \,. \tag{9.37}$$

9.4: For 4-level PAM where the transmitted pulse level dz_n at time nT takes on the values [–3, –1, 1, 3] with equal probability, and with the $\{d_n\}$ mutually uncorrelated, derive the reference signal covariance matrix

$$R = E\{\mathbf{d}_n \mathbf{d}_n'\} .$$

9.5: Determine the values of the coefficients K_n^c, $n = 0, \ldots, N-1$, which minimize $E(e_i^2)$ where e_i is the echo estimation error, given by (9.100), for the lattice filter.

9.6: Let P be the matrix of column eigenvectors of the covariance matrix R, i.e., $R p_j = \lambda_j p_j$, p_j the jth column of P.

(a) Show that $PP' = I$, i.e., P is orthonormal.

(b) Show that $[I - \beta R]^n = P[1 - \beta]^n P'$.

9.7: Show that an echo canceler tap-weight set equal to samples, at Nyquist interval T', of the echo channel $h_e(t)$ minimizes the mean-squared cancellation error, provided the local and distant data trains are uncorrelated.